JACS
JOURNAL OF THE AMERICAN CHEMICAL SOCIETY

Communication

pubs.acs.org/JACS

Structurally Defined Graphene Nanoribbons with High Lateral Extension

Matthias Georg Schwab,[†,§] Akimitsu Narita,[†] Yenny Hernandez,[†,∥] Tatyana Balandina,[‡] Kunal S. Mali,[‡] Steven De Feyter,[‡] Xinliang Feng,[†] and Klaus Müllen*[,†]

[†]Max Planck Institute for Polymer Research, Ackermannweg 10, D-55128 Mainz, Germany

[‡]Division of Molecular and Nanomaterials, Department of Chemistry, and INPAC-Institute of Nanoscale Physics and Chemistry, Katholieke Universiteit Leuven, Celestijnenlaan, 200 F, B 3001 Leuven, Belgium

Supporting Information

ABSTRACT: Oxidative cyclodehydrogenation of laterally extended polyphenylene precursor allowed bottom-up synthesis of structurally defined graphene nanoribbons (GNRs) with unprecedented width. The efficiency of the cyclodehydrogenation was validated by means of MALDI-TOF MS, FT-IR, Raman, and UV−vis absorption spectroscopies as well as investigation of a representative model system. The produced GNRs demonstrated broad absorption extended to near-infrared region with the optical band gap of as low as 1.12 eV.

Graphene nanoribbons (GNRs), characterized by a large aspect ratio with lateral quantum confinement, are predicted to possess a band gap[1−5] in contrast to graphene which itself is a zero band gap semimetal.[6] It has been theoretically and experimentally demonstrated that both width and edge structure of GNRs strongly govern the electronic characteristics of graphene materials.[1,7,8] Their appealing electronic properties can only be accessed, however, if new methods for reliable and reproducible build-up of well-defined GNRs with precise lateral and longitudinal dimensions are developed. Top-down approaches such as lithographic "cutting" of graphene,[1,2] longitudinal "unzipping"[3] or "etching"[4] of carbon nanotubes, and the surfactant-assisted extraction from graphite dispersions[5] cannot reach the required chemical precision. In our search for synthetic pathways toward GNRs, we have worked out a bottom-up strategy that relies on the intramolecular oxidative cyclodehydrogenation[9,10] of tailored polyphenylene precursors.[11−15] Hence, a number of different GNR geometries have been realized, ranging from fully linear[11,14,15] to kinked.[12,13,15] The versatility of this method was successfully demonstrated both for solution-[11−14] and surface-based[15] protocols, resulting in GNRs of atomic accuracy. This stands in sharp contrast to the aforementioned top-down methods.[1−5]

GNRs so far fabricated by bottom-up approaches are limited to those with lateral dimensions smaller than 1 nm, which show absorption only up to 670 nm and calculated band gap larger than 1.6 eV.[11−15] For future applications in electronic devices, it is essential to synthesize GNRs with tailored band gaps. In this work, we present a solution synthesis and characterization of unprecedentedly broad, low band gap, and structurally defined GNRs, which can be derived from laterally extended polyphenylene precursors. For comparison, a representative model polycyclic aromatic hydrocarbon (PAH, **C78**,[16,17] with 78 carbon atoms in the aromatic core) of GNRs is also reported, for which a new efficient synthesis is validated by means of matrix-assisted laser desorption/ionization time-of-flight (MALDI-TOF) mass spectrometry (MS), ^{1}H NMR spectroscopy, and scanning tunneling microscope (STM).

First, *para*-terphenyl-based oligophenylene precursor **4a**, which corresponds to target PAH **C78**,[16,17] was designed as a model compound to examine its suitability for efficient cyclodehydrogenation (Scheme 1). Synthesis of **4a** was initiated with *Sonogashira-Hagihara* cross-coupling of 2,2″-diiodoterphenyl **1a** with trimethylsilyl acetylene followed by deprotection to yield 2,2″-diethynylterphenyl **2a**. Two-fold Diels−Alder cycloaddition between **2a** and functionalized tetraphenylcyclopentadienone **3**[18] under microwave conditions effi-

Scheme 1. Synthetic Route to PAH C78 and GNR 6[a]

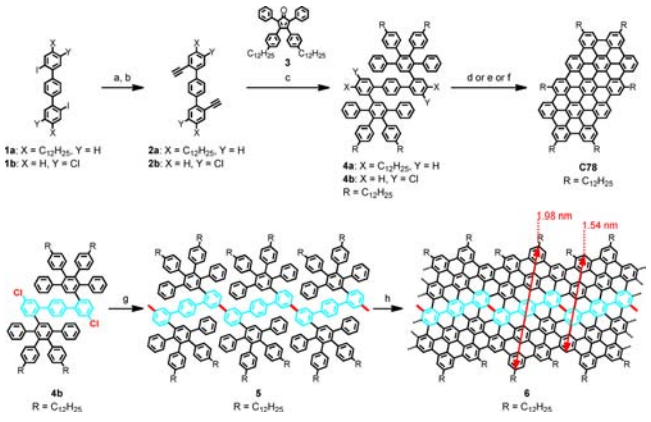

[a]Geometric dimensions of GNR **6** were derived from Merck Molecular Force Field 94 (MMFF94) calculations. Reagents and conditions: (a) trimethylsilyl acetylene, $Pd(PPh_3)_2Cl_2$/CuI, NEt_3, rt; (b) K_2CO_3, THF/MeOH, rt, **2a**: 51% (two steps), **2b**: 58% (two steps); (c) xylene, 160 °C, μW, 300 W, **4a**: 81%, **4b**: 85%; (d) $FeCl_3$, CH_2Cl_2/CH_3NO_2, rt, 93%; (e) $MoCl_5$, CH_2Cl_2, rt, 85%; (f) PIFA/BF_3, CH_2Cl_2, −60 °C, then −10 °C, 81%; (g) bis(cycloocta-(1,5)-diene)nickel(0) cycloocta-(1,5)-diene, 2,2′-bipyridine, toluene/DMF, 80 °C, 81%; (h) $FeCl_3$, CH_2Cl_2/CH_3NO_2, rt, 92%.

Received: August 3, 2012
Published: October 19, 2012

   dx.doi.org/10.1021/ja307697j | J. Am. Chem. Soc. 2012, 134, 18169−18172

ciently produced **4a** in 81% yield. Subsequent experiments confirmed that **4a** can be readily transformed into **C78** by using either the established $FeCl_3$ mediated cyclodehydrogenation[9,10,16,17] or less common oxidative procedures involving $MoCl_5$[10,19] or PIFA/BF_3.[10,18] In all three cases, characterization of the products by a combination of MALDI-TOF MS and ^{1}H NMR spectroscopy proved the formation of **C78** as an exclusive product (Figures 1 and S1). No partially fused

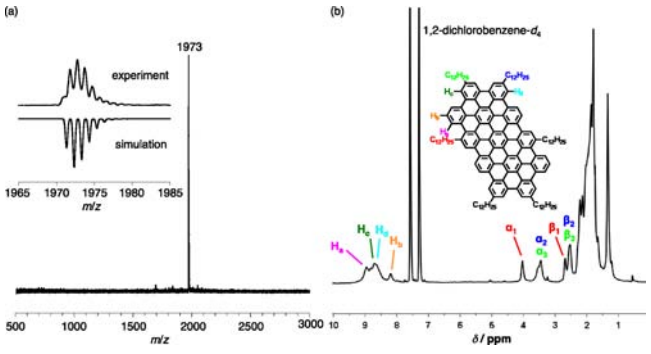

Figure 1. (a) MALDI-TOF MS spectrum of **C78**; inset: the isotopic distribution is in agreement with the simulated result. (b) ^{1}H NMR spectrum of **C78** in 1,2-dichlorobenzene-d_4 at 170 °C.

intermediates or chlorinated products could be detected by MALDI-TOF MS, and comparison of the isotropic distribution with simulation proved the complete cyclodehydrogenation (Figure 1a). Generally, PAHs suffer from strong aggregation in solution, which results in broadening of peaks in ^{1}H NMR spectroscopy.[20] Remarkably, however, a well resolved ^{1}H NMR spectrum could be recorded for **C78** at 170 °C by using high-boiling-point solvent, 1,2-dichlorobenzene-d_4 (Figure 1b). Because of its extended π-system, the signals of the protons on the aromatic backbone of **C78** appeared strongly downfield shifted in a range between δ = 8.0 and 9.5 ppm. With the help of peak integration and Nuclear *Overhauser* enhancement spectroscopy (NOESY) measurements, a number of aliphatic and aromatic signals could be assigned as indicated in Figure 1b, which further confirmed the chemical identity of the product. To our best knowledge, this is the largest PAH that allows for structural characterization by ^{1}H NMR.

Furthermore, STM rendered the visualization of **C78** at the solid–liquid interface of Au(111)/1,2,4-trichlorobenzene (TCB) (Figure 2a). The alkyl chains were surface-crystallized and split into a set of four lateral and two kinked longitudinal

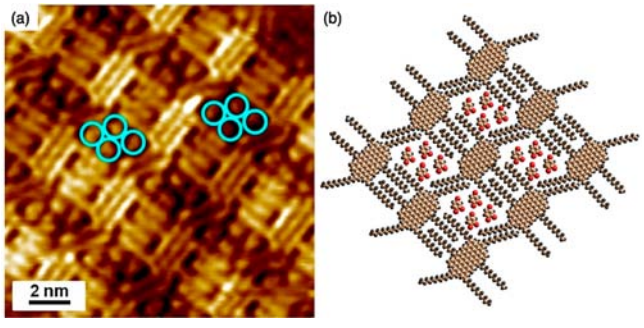

Figure 2. (a) STM image of **C78** physisorbed at the Au(111)/TCB interface; blue circles indicate entrapped guest molecules; imaging conditions: I_t = 0.1 nA, V_{bias} = 464 mV. (b) A tentative molecular model for the self-assembly of **C78** on Au (111).

chains. The aromatic core showed three parallel stripes running along the long axis, which correlated with electron densities in the highest occupied molecular orbitals.[17] The dimensions of the core extracted from the image (length = 2.3 ± 0.1 nm and width 1.4 ± 0.1 nm) were in good agreement with the values obtained by molecular modeling (Figure 2b). The remaining interspace between four **C78** molecules was filled with TCB guest molecules that appeared as small bright spots. These observations clearly support the defect-free synthesis of **C78** (see Supporting Information for more details). It should be mentioned here that, despite the successful synthesis of **C78** in previous reports,[16,17] the present protocol shows the obvious advantage regarding the cyclodehydrogenation efficiency of precursors that can avoid the rearrangement under the experimental conditions. More importantly, precursor **4** can be considered as a repeating unit of polyphenylene precursor **5** which renders one to produce laterally extended GNR **6** with a width of 1.54–1.98 nm (Scheme 1).

So far, all chemical routes toward the synthesis of polyphenylene precursors made use of A_2B_2-type polycondensation reactions such as *Suzuki-Miyaura* cross-coupling[11,12] and *Diels–Alder* reaction.[13,14] Because of the intrinsic sensitivity of these protocols to stoichiometry,[21] an *AA*-type *Yamamoto* polycondensation system which can circumvent this drawback is believed to be more efficient and can yield high molecular-weight precursors. Therefore, monomer **4b** substituted with reactive halogen groups was synthesized, allowing an *AA*-type Yamamoto polymerization to yield kinked polyphenylene precursor **5** (Scheme 1).[21] MALDI-TOF MS characterization of **5** indicated the presence of a regular pattern with molecular weight up to 35 000–40 000 g mol^{-1} (Figure 3a). On this basis,

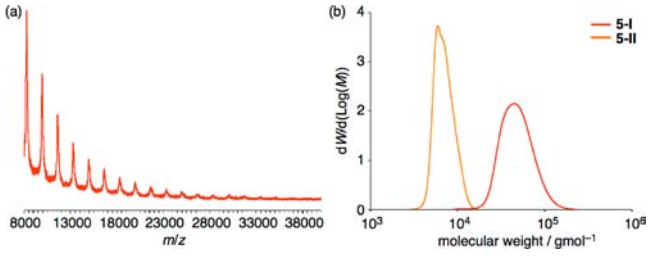

Figure 3. (a) Linear-mode MALDI-TOF MS spectra of polyphenylene precursor **5** (before separation). (b) Molecular weight distribution of **5-I** and **5-II** (SEC, eluent: THF, PS standard).

the number of repeating units in **5** was 21–24, which corresponded to approximately 30 nm of the resultant GNRs. This is most likely not the maximal value, however, due to the limitation of MALDI-TOF MS for the analysis of high-molecular-weight species with a broad molecular weight distribution.[12,22] Further investigation of **5** by size exclusion chromatography (SEC) revealed its relatively high polydispersity index (PDI) of 2.2. Therefore, the crude polymer **5** was separated into two fractions by utilizing preparative SEC. The fraction of larger molecular weight **5-I** showed weight-average molecular weight (M_w) of 52 000 g mol^{-1} with PDI of 1.2, whereas the other fraction of smaller molecular weight **5-II** showed M_w of 7200 g mol^{-1} with PDI of 1.1 (Figure 3b). These results based on SEC are approximately relative values according to the polystyrene (PS) standard calibration,[23] but they highlight the superiority of the *AA*-type Yamamoto approach over the A_2B_2-type polymerization for the preparation of high molecular weight precursors.[11–13]

dx.doi.org/10.1021/ja307697j | J. Am. Chem. Soc. 2012, 134, 18169–18172

Next, intramolecular cyclodehydrogenation of precursors **5**, **5-I**, and **5-II** was performed using $FeCl_3$ as oxidant in a mixture of dichloromethane and nitromethane, yielding GNRs **6**, **6-I**, and **6-II**, respectively. MALDI-TOF MS analysis of GNR **6-II** suggested a similar number of repeating units with respect to precursor **5-II** (Figure S11). However, GNRs **6** and **6-I** were precluded from MALDI-TOF MS characterization possibly owing to the strong aggregation of high molecular weight GNRs.[19,22]

Fourier transform infrared (FTIR) spectroscopy analysis of precursor **5** and GNR **6** showed the disappearance of the band at 4050 cm^{-1} which originates from the rotation of free phenyl rings (Figure 4).[13,24] Further, the signal triad at 3025, 3056, and

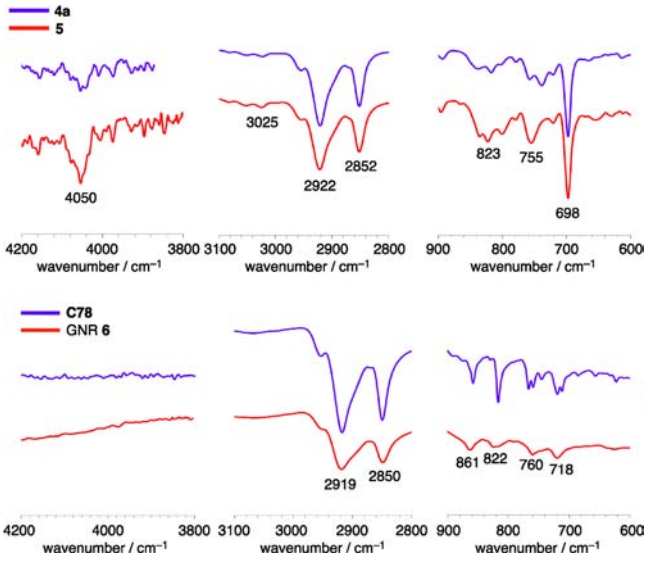

Figure 4. Representative FTIR spectral regions before (**4a**, **5**) and after (**C78**, GNR **6**) oxidative cyclodehydrogenation.

3083 cm^{-1} which is typical for aromatic C−H stretching vibrations was diminished, and the fingerprint bands at 698 and 755 cm^{-1} originating from monosubstituted benzene rings were attenuated.[24,25] These observations were in line with the analogous conversion of model compound **4a** into **C78**, and indicated highly efficient "graphitization" of precursor **5** into GNR **6**. Raman spectrum of a powder sample of GNR **6-I** was measured at 488 nm with laser power of 1 mW, and showed first-order D band (disorder band) and G band (graphite band) at 1316 and 1595 cm^{-1}, respectively, consistent with literature values for GNRs (Figure 5a).[3,4,15,26] The relatively high intensity of the D band could be explained by the contribution of the edges as defects.[4,12,15,26] Moreover, well-resolved double-resonant signals were also observed at 2632, 2910, and 3194 cm^{-1}, which could be assigned to 2D, D+G, and 2G bands, respectively.[26] It should be mentioned that the G* band (~2450 cm^{-1}) typical for graphene was apparently too small to be observed, because a powder (multilayer) sample was used for the measurement in this work.[26d]

The GNR samples were virtually insoluble in conventional organic solvents such as dichloromethane, chloroform, and toluene. However, use of *N*-methylpyrrolidone (NMP), which is known as a good solvent for the exfoliation of graphene[27] as well as for the debundling of carbon nanotubes,[28] enabled the exfoliation of GNRs with the assistance of mild sonication to obtain stable dispersions (~60 μg/mL) (Figure 5b, inset).

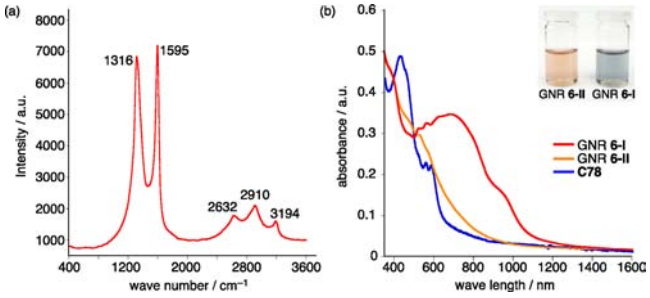

Figure 5. (a) Raman spectrum of GNR **6-I** measured at 488 nm (powder, laser power: 1 mW). (b) Normalized UV−vis absorption spectra of GNR **6-I** (red, in NMP), GNR **6-II** (orange, in NMP), and **C78** (blue, in THF); inset: a picture of solutions of GNR **6-I** and **6-II** in NMP.

Thus, UV−vis absorption spectra of GNR **6-I** and **6-II** were recorded in NMP and compared with that of **C78** (17 μM in THF) as shown in Figure 5b. For **C78**, the β-band was observed at 431 nm and the p- and α-band were located at 514 and 580 nm, respectively. The relatively high intensity of the α-band could be attributed to the low symmetry of **C78**.[18,29] The optical band gap of **C78** could not be determined from the onset of the p-band due to the broadened absorption bands,[29] but was estimated to be larger than 1.92 eV from the absorption edge of 647 nm. It is remarkable to note that the longest GNR **6-I** showed absorption peaks at 690 and 960 nm with broad absorption extended to the near-infrared (NIR) region. The absorption edges of GNR **6-I** and **6-II** were derived from the spectra to be 1109 and 812 nm, corresponding to the optical band gap of 1.12 and 1.53 eV, respectively. Thereby, this result undoubtedly demonstrated the extraordinarily low band gap of the laterally extended GNRs compared to previously bottom-up synthesized GNRs.[11−15] Furthermore, the optical band gap of 1.12 eV is in a good agreement with the calculated band gap of 1.08 eV, proving that GNR **6-I** is sufficiently elongated, namely more than 15 repeating units, or approximately 20 nm, to obtain the lowest band gap achievable with its lateral structure.[30]

In summary, structurally defined and laterally extended GNRs were synthesized via a bottom-up chemical approach. Characterizations by MALDI-TOF MS, FTIR, Raman, and UV−vis absorption spectroscopies as well as investigation of a model system validated the efficiency of the cyclodehydrogenation. For the first time, it was possible to access GNRs with band gap as low as 1.12 eV, reaching a broad absorption up to the NIR region. These GNRs may hold the potential in a number of opoelectronic devices such as solar cell, optical switching, and infrared imaging.

■ ASSOCIATED CONTENT

Supporting Information

Experimental details, NMR, MALDI-TOF MS, UV−vis absorption, fluorescence, and DSC spectra. This material is available free of charge via the Internet at http://pubs.acs.org.

■ AUTHOR INFORMATION

Corresponding Author

muellen@mpip-mainz.mpg.de

Present Addresses

[§]BASF SE, Carl-Bosch-Strasse 38, 67056 Ludwigshafen, Germany

[‖]Physics Department, Universidad de los Andes, Carrera 1 18A-10, Bloque Ip. Bogotá, Colombia

Notes

The authors declare no competing financial interest.

■ ACKNOWLEDGMENTS

We are grateful to the financial support from ERC grant on NANOGRAPH, EU Project SUPERIOR (PITN-GA-2009-238177) and GENIUS, DFG Priority Program SPP 1459, ESF Project GOSPEL (Ref Nr: 09-EuroGRAPHENE-FP-001), the Max Plank Society through the program ENERCHEM, DFG Priority Program SPP 1355, DFG MU 334/32-1.

■ REFERENCES

(1) Han, M. Y.; Özyilmaz, B.; Zhang, Y.; Kim, P. *Phys. Rev. Lett.* **2007**, *98*, 206805.
(2) (a) Özyilmaz, B.; Jarillo-Herrero, P.; Efetov, D.; Kim, P. *Appl. Phys. Lett.* **2007**, *91*, 192107. (b) Jia, X.; Hofmann, M.; Meunier, V.; Sumpter, B. G.; Campos-Delgado, J.; Romo-Herrera, J. M.; Son, H.; Hsieh, Y. P.; Reina, A.; Kong, J. *Science* **2009**, *323*, 1701.
(3) (a) Kosynkin, D. V.; Higginbotham, A. L.; Sinitskii, A.; Lomeda, J. R.; Dimiev, A.; Price, B. K.; Tour, J. M. *Nature* **2009**, *458*, 872. (b) Shimizu, T.; Haruyama, J.; Marcano, D. C.; Kosinkin, D. V.; Tour, J. M.; Hirose, K.; Suenaga, K. *Nat. Nanotechnol.* **2011**, *6*, 45.
(4) Jiao, L.; Zhang, L.; Wang, X.; Diankov, G.; Dai, H. *Nature* **2009**, *458*, 877.
(5) Li, X.; Wang, X.; Zhang, L.; Lee, S.; Dai, H. *Science* **2008**, *319*, 1229.
(6) (a) Wallace, P. R. *Phys. Rev. Lett.* **1947**, *71*, 622. (b) Castro Neto, A. H.; Guinea, F.; Peres, N. M. R.; Novoselov, K. S.; Geim, A. K. *Rev. Mod. Phys.* **2009**, *81*, 109.
(7) (a) Schwierz, F. *Nat. Nanotechnol.* **2010**, *5*, 487. (b) Chen, Z.; Lin, Y. M.; Rooks, M. J.; Avouris, P. *Physica E* **2007**, *40*, 228.
(8) (a) Barone, V.; Hod, O.; Scuseria, G. E. *Nano Lett.* **2006**, *6*, 2748. (b) Yang, L.; Park, C.-H.; Son, Y.-W.; Cohen, M. L.; Louie, S. G. *Phys. Rev. Lett.* **2007**, *99*, 186801. (c) Radovic, L. R.; Bockrath, B. *J. Am. Chem. Soc.* **2005**, *127*, 5917.
(9) Scholl, R.; Seer, C. *Liebigs Ann. Chem.* **1912**, *394*, 111.
(10) Rempala, P.; Kroulík, J.; King, B. T. *J. Am. Chem. Soc.* **2004**, *126*, 15002.
(11) Yang, X.; Dou, X.; Rouhanipour, A.; Zhi, L.; Räder, H. J.; Müllen, K. *J. Am. Chem. Soc.* **2008**, *130*, 4216.
(12) Dössel, L.; Gherghel, L.; Feng, X.; Müllen, K. *Angew. Chem., Int. Ed.* **2011**, *50*, 2540.
(13) Wu, J.; Gherghel, L.; Watson, M. D.; Li, J.; Wang, Z.; Simpson, C. D.; Kolb, U.; Müllen, K. *Macromolecules* **2003**, *36*, 7082.
(14) Fogel, Y.; Zhi, L.; Rouhanipour, A.; Andrienko, D.; Räder, H. J.; Müllen, K. *Macromolecules* **2009**, *42*, 6878.
(15) Cai, J.; Ruffieux, P.; Jaafar, R.; Bieri, M.; Braun, T.; Blankenburg, S.; Muoth, M.; Seitsonen, A. P.; Saleh, M.; Feng, X.; Müllen, K.; Fasel, R. *Nature* **2010**, *466*, 470.
(16) (a) Müller, M.; Iyer, V. S.; Kübel, C.; Enkelmann, V.; Müllen, K. *Angew. Chem., Int. Ed.* **1997**, *36*, 1607. (b) Morgenroth, F.; Kübel, C.; Müller, M.; Wiesler, U. M.; Berresheim, A. J.; Wagner, M.; Müllen, K. *Carbon* **1998**, *36*, 833.
(17) Böhme, T.; Simpson, C.; Müllen, K.; Rabe, J. *Chem.—Eur. J.* **2007**, *13*, 7349.
(18) Takada, T.; Arisawa, M.; Gyoten, M.; Hamada, R.; Tohma, H.; Kita, Y. *J. Org. Chem.* **1998**, *63*, 7698.
(19) Kramer, B.; Fröhlich, R.; Waldvogel, S. *Eur. J. Org. Chem.* **2003**, 3549.
(20) (a) Wasserfallen, D.; Kastler, M.; Pisula, W.; Hofer, W. A.; Fogel, Y.; Wang, Z.; Müllen, K. *J. Am. Chem. Soc.* **2006**, *128*, 1334. (b) Kastler, M.; Pisula, W.; Wasserfallen, D.; Pakula, T.; Müllen, K. *J. Am. Chem. Soc.* **2005**, *127*, 4286.
(21) (a) Carothers, W. H. *Trans. Faraday Soc.* **1936**, *32*, 39. (b) Odian, G. G. *Principles of Polymerization*; J. Wiley & Sons: Hoboken, NJ, 2004.
(22) Martin, K.; Spickermann, J.; Räder, H. J.; Müllen, K. *Rapid Commun. Mass Spectrom.* **1996**, *10*, 1471.
(23) The PS standard was used for the SEC analysis instead of the poly(*para*-phenylene) standard, considering the kinked and nonrigid structure of polyphenylene precursor **5**.
(24) Centrone, A.; Brambilla, L.; Renouard, T.; Gherghel, L.; Mathis, C.; Müllen, K.; Zerbi, G. *Carbon* **2005**, *43*, 1593.
(25) Shifrina, Z. B.; Averina, M. S.; Rusanov, A. L.; Wagner, M.; Müllen, K. *Macromolecules* **2000**, *33*, 3525.
(26) (a) Malard, L. M.; Pimenta, M. A.; Dresselhaus, G.; Dresselhaus, M. S. *Phys. Rep* **2009**, *473*, 51. (b) Ryu, S.; Maultzsch, J.; Han, M. Y.; Kim, P.; Brus, L. E. *ACS Nano* **2011**, *5*, 4123. (c) Bischoff, D.; Güttinger; Dröscher, S.; Ihn, T.; Ensslin, K.; Stampfer, C. *J. Appl. Phys.* **2011**, *109*, 073710. (d) Yoon, D.; Moon, H.; Cheong, H.; Choi, J. S.; Choi, J. A.; Park, B. H. *J. Korean Phys. Soc.* **2009**, *55*, 1299.
(27) Hernandez, Y.; Nicolosi, V.; Lotya, M.; Blighe, F. M.; Sun, Z.; De, S.; McGovern, I. T.; Holland, B.; Byrne, M.; Gun'Ko, Y. K.; Boland, J. J.; Niraj, P.; Duesberg, G.; Krishnamurthy, S.; Goodhue, R.; Hutchison, J.; Scardaci, V.; Ferrari, A. C.; Coleman, J. N. *Nat. Nanotechnol* **2008**, *3*, 563.
(28) Bergin, S. D.; Nicolosi, V.; Streich, P. V.; Giordani, S.; Sun, Z.; Windle, A. H.; Ryan, P.; Niraj, N. P. P.; Wang, Z.-T. T.; Carpenter, L.; Blau, W. J.; Boland, J. J.; Hamilton, J. P.; Coleman, J. N. *Adv. Mater.* **2008**, *20*, 1876.
(29) Rieger, R.; Müllen, K. *J. Phys. Org. Chem.* **2010**, *23*, 315.
(30) Osella, S.; Narita, A.; Schwab, M. G.; Hernandez, Y.; Feng, X.; Müllen, K.; Beljonne, D. *ACS Nano* **2012**, *6*, 5539.